Multi-frequency sweeping interferometry using spatial optical frequency modulation

Samuel Choi[a], Heiichi Kato[b], Osami Sasaki[a], and Takamasa Suzuki[b]
[a] Department of Electrical and Electronic Engineering, Niigata University, 8050 Ikarashi-2 Niigata, Japan; [b] Graduate School of Engineering, Niigata University, 8050 Ikarashi-2 Niigata, Japan.

ABSTRACT

We investigated the interference amplitude and phase characteristics of a multi-frequency sweeping interferometer with sinusoidal phase modulating technique. A novel multi frequency sweeping light source that generated an interval and center frequency variable frequency comb with a bandwidth of 14 nm was demonstrated. The interference phase and amplitude distributions were investigated by observing the zeroth and first order interference signals. In addition, the zeroth and first order interference phase variations caused by center frequency sweeping were measured.

Keywords: Interferometry, Multiple-frequency sweeping, Optical frequency comb, Spatial light modulation, Interference phase measurement

1. INTRODUCTION

Optical frequency combs (OFCs) produced by a femtosecond pulse lasers have been used to precisely measure long distances based on their characteristics of a multi-frequency spectrum [1–3]. However, they are not suitable for compact interferometers used for surface profile and thickness measurements because OFCs have a low interval frequency of tens of MHz and fixation of the interval frequency. Recently, a multi-frequency spectral-domain interferometer for thickness and refractive index measurements of silicon wafers [4] and ultrahigh-scanning speed optical coherence tomography using two OFC generators [5] have been demonstrated. The former technique requires signal processing involving taking the Fourier transform to extract the peak position of the interference amplitude. The latter technique requires using two synchronized OFC generators to produce the Vernier effect. Since these light sources consist of a phase modulator installed in a Fabry–Perot cavity, the interval frequency is fixed because it is driven by an integer multiple of the cavity free spectral range (FSR).

On the other hand, a novel profilometer has been demonstrated that employs interval-frequency-variable multi-frequency interferometry [6]. The supercontinuum produced by an optical pulse synthesizer was utilized to improve the depth resolution of this profilometer [7]. These techniques can realize a depth scan range of several meters without mechanical scanning because the phase-modulated light source can sweep the interval frequency since it is not limited by the cavity FSR. In addition, higher-order interference peaks permit long distances to be measured without extending the reference arm. However, this technique has a depth resolution of only a few tens of micrometers because only the interference amplitude is used to measure distances; interference phase information has not been considered in such interferometry. Unless the measurement object is a scattering medium such as biological tissue, it is preferable to utilize the interference phase near the interference amplitude peak to accurately measure the distance of a reflecting object. However, the characteristics of the interference phase have not been experimentally determined.

We demonstrate a new scheme for a multi-frequency sweeping light source with a spatial frequency filter (SFF) replacing the conventional OFCs. This light source can easily generate a broad bandwidth by using a low-coherence light source and by sweeping both the center and interval frequencies by controlling the SFF. The dependencies of the interference amplitude and the phase on the center and interval frequencies are examined experimentally to confirm the theoretical principle of multi-frequency sweeping interferometry. The amplitude and phase of the zeroth- and first-order interference signals are calculated by sinusoidal phase modulating (SPM) technique [8].

*schoi@eng.niigata-u.ac.jp; phone 81 25 262-6761;

Optical Metrology and Inspection for Industrial Applications II, edited by Kevin G. Harding, Peisen S. Huang, Toru Yoshizawa, Proc. of SPIE Vol. 8563, 856302 · © 2012 SPIE
CCC code: 0277-786/12/$18 · doi: 10.1117/12.999555

2. PRINCIPLE

The interference signal produced by the multi-frequency is regarded as a superposition of the interference signals produced by each frequency component. Therefore, the resulting interference signal is expressed by

$$S(\Delta f, f_c) = \sum_{m=0}^{\infty} F(m\Delta f)\cos\{2\pi(f_c \pm m\Delta f)L/c\} \quad (1),$$
$$= 2\left(\sum_{m=0}^{\infty} F(m\Delta f)\cos(2\pi m\Delta f L/c)\right)\cos(2\pi f_c L/c)$$

where Δf is the interval frequency, f_c is the center frequency, and L is the optical path difference (OPD) of the interferometer. $F(m\Delta f)$ is the interference amplitude of each frequency component, where m is the number of longitudinal modes of the multi-frequency. The line width of the longitudinal modes is ignored for simplicity. The interval frequency is symmetrically swept on either side of the center frequency. Equation (1) can be simplified by considering the Fourier series expansion of an even function:

$$S(\Delta f, f_c) = B(L - Nc/\Delta f)\cos(\alpha), \quad (2),$$
$$\alpha = 2\pi f_c L/c, N = 1,2,..,$$

where the amplitude term B is the real part of the inverse Fourier transform of $F(m\Delta f)$ and N is the order of the interference amplitude peak. For simplicity, the envelope of the spectrum $F(m\Delta f)$ is assumed to be a Gaussian function with a bandwidth of f_B; thus, $B=B_0\exp\{-4\ln 2(L-Nc/2\Delta f)^2/L_{res}^2\}$, where the depth resolution $Lres \approx 2\ln 2 c/\pi f_B$. The interference amplitude has its peak value whenever the interval frequency satisfies the condition $\Delta f=\Delta f_N=Nc/L_N$ as Δf is swept. L_N is the higher-order peak position of the OPD

The interference amplitude peak value $S(\Delta fN)=B_0\cos(\alpha)$ is a function of the interference phase α. Figure 1 shows the dependence of the interference amplitude and phase distributions on the interval frequency. As shown in Eq. (2), the interference amplitude and phase can be independently controlled by Δf and fc, respectively. The interference phase at the Nth-order amplitude peak position is $\alpha N=2\pi Nfc/\Delta f_N$, as shown in Fig. 1. When fc is an integer multiple of Δf_N, α_N will be identical to zero because α_N becomes an integer multiple of 2π, as shown in Fig. 2. If f_c is shifted from $p\Delta f_N$ to $p\Delta f_N+\delta f$ (where p is an integer), then αN will shift by $2\pi N\delta f/\Delta f_N$. This implies that the interference phase can be controlled by shifting the center frequency.

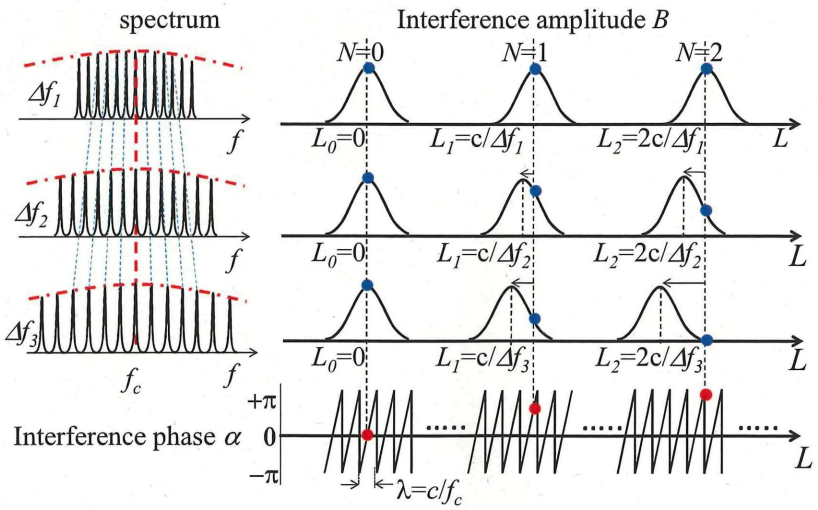

Fig. 1 Dependence of the interference amplitude on the interval frequency Δf.

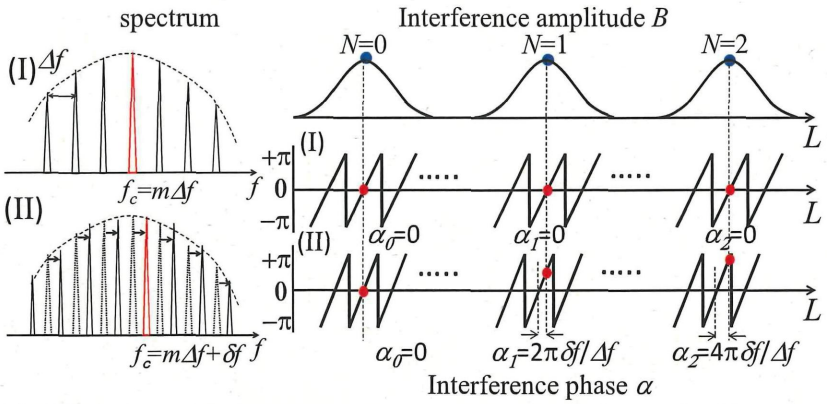

Fig. 2 Dependence of the interference phase shift on the center frequency of multi-frequency.

3. EXPERIMENTAL SETUP

Figure 3 shows a schematic of the experimental setup. The light source consists of a superluminescent diode (SLD) with a collimator, a telecentric optical system with a SFF, and a pair of diffraction gratings (DG1, 2). The center wavelength and full width at half maximum (FWHM) bandwidth of the SLD were 844.4 nm and approximately 15 nm, respectively. The collimated beam was diffracted by the DG1. The first-order diffracted light was focused by L1 and it formed a spatial optical spectrum on the focal plane where the SFF was introduced to select the frequency components to generate the multi-frequency spectrum. A star-like Ronchi-ruling target with a mask whose resolution varied from 10 to 100 lp/mm in the z direction was utilized as the SFF. The transmittance distribution of the SFF was a rectangular array with a duty ratio of 50 %. Thus, the SFF had a finesse of approximately 1. Consequently, interference signals with orders higher than two had low intensities, making them difficult to detect. However, this method has the advantages that a wide bandwidth can be easily obtained from a white-light source and that the interval and center frequencies can be swept with no limitation on the sweeping range. The output spectrum was fabricated by superimposing the frequency components using the DG2. The FWHM bandwidth f_B was about 14 nm. The center and interval frequencies could be swept by moving the SFF in the y and z directions, respectively. The input light was split into the two beams by a beam splitter (BS) and these beams were reflected by mirrors M1 and M2, respectively, to interfere with each other. M1 was vibrated sinusoidally by a piezoelectric transducer (PZT) to perform SPM interferometry. A sinusoidal phase-modulated interference signal was detected by a two-dimensional CCD and SPM interferometry accurately measured the amplitude and phase of the interference signal.

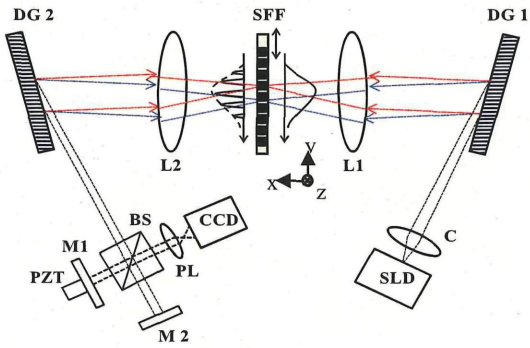

Fig. 3 Schematic of multi-frequency sweeping interferometer (C: collimator; DG1 and 2: diffraction gratings; SFF: spatial frequency filter; L1 and 2: lenses; M1 and 2: plane mirrors; PZT: piezoelectric transducer; BS: beam splitter; PL: projection lens; CCD: charge-coupled device image sensor).

4. RESULT

In this experiment, we obtained a multi-frequency spectrum with the frequency spacing of 1.2 x 102 GHz and bandwidth of 27 nm as shown in Figure.3. The generated multi-frequency light enters the Michelson interferometer to observe the interferometric characteristics. The reference mirror is vibrated by PZT with 50 Hz to carry out the SPM. The CCD image sensor captures the 2-dimensional interferometric signals with the frame rate of 400 Hz which is eight time of SPM frequency.

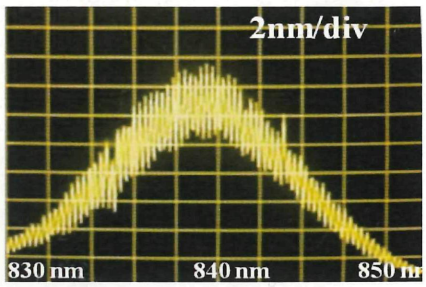

Fig.3 Resulting multi-frequency spectrum

Figure 4 shows the zeroth- and first-order interference amplitudes when the interval frequency was swept by moving the SFF in the z direction. A sweeping distance of 14 mm provided an interval frequency sweep of about 4 THz. The ratio of the sweeping distance to the interval frequency sweep was approximately –275.5 GHz/mm. The zeroth-order interference amplitude was almost constant, whereas the first-order interference amplitude had a peak value when the interval frequency Δf was 2.8 THz. The OPD was calculated to be L1=106.5 μm from L1=c/Δf. The peak width of the first-order amplitude distribution was about 22.5 μm, which agreed with the theoretical value estimated using Lres≈2ln2c/πfB, where fB=5.9 THz.

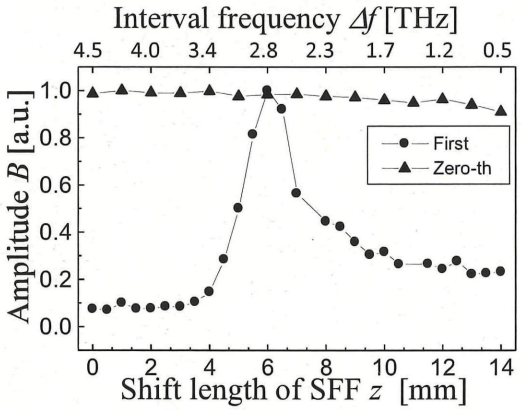

Fig. 4 The zeroth- and first-order interference amplitudes as a function of shift of SFF in the z direction and corresponding interval frequency.

Figures 5(a) and (b) show the first-order interference amplitude and phase distributions near the amplitude peak position, respectively. As shown in Fig. 5(b), the interference phase remained almost constant as the interval frequency was swept. The measured phase fluctuated slightly because the center frequency was not completely fixed since the SFF was mechanically moved in the z direction. However, the experimental results reveal that the interference phase was almost constant over a sweeping width of 500 GHz. This means that the interval frequency was swept independently of the center frequency by the SFF. The experimental result in Fig. 5 was obtained due to fc and Δf being independent.

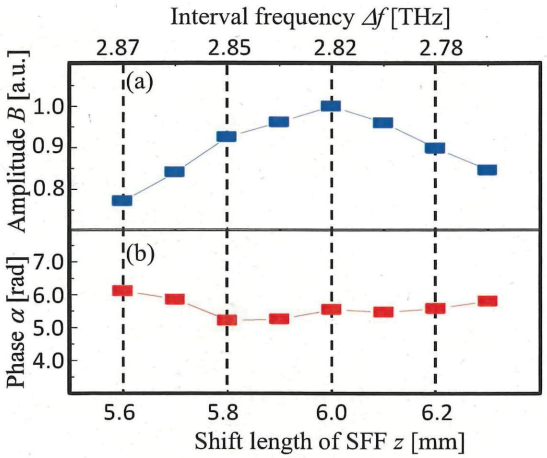

Fig. 5. First-order interference (a) amplitude, and (b) phase distributions near the amplitude peak position as a function of shift length of SFF in the z direction and corresponding interval frequency

Figure 6 shows the surface profile of M2 in Fig.2 obtained from unwrapped phase distribution detected by SPM using the first-order interferometric peak. The M2 was set to be 1.3 mm away from zero-OPD position. This means that the displacement of object with step height longer than the wavelength can be measured without reference mirror scanning. Figure 7(a) and (b) show the shift of the phase distributions of the mirror surface obtained from zeroth- and first-order interferometric peaks respectively, when the spatial filter was slightly moved to sweep the center frequency of the OFC.

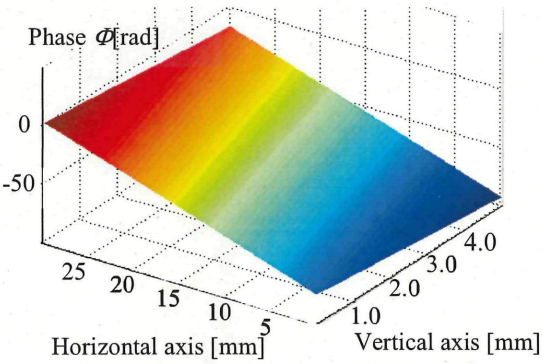

Fig. 6 Surface profile of the mirror

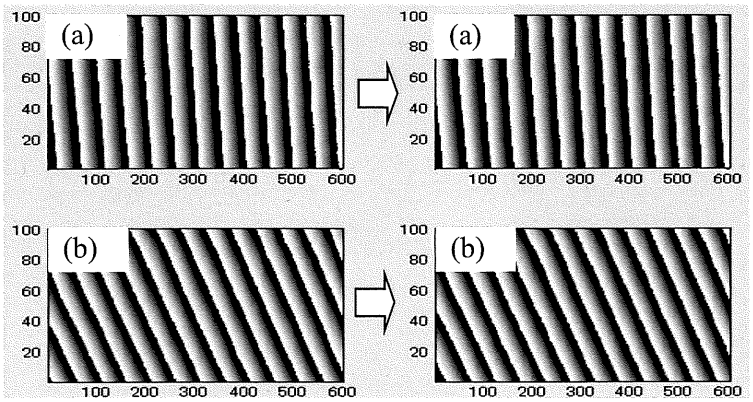

Fig. 7 Phase distributions in the case of (a) 0th order and (b) first order interferometric signals.

The center frequency was swept by moving the SFF in the y direction in increments of 12.5 μm. Since the interval frequency was almost fixed at 120 GHz, the amplitude peak positions did not change. Figure 8 shows the values of the interference phase at the amplitude peak positions of the zeroth and first order interference signals. For the zeroth-order interference signal, the interference phase was constant. In contrast, the interference phase of the first-order interference signal shifted by 4π for SFF movement of 300 μm, which corresponds to sweeping the center frequency by 240 GHz. This result demonstrates that the interference phase at the amplitude peak position fixed by the constant interval frequency could be changed independently by sweeping the center frequency, as shown in Fig. 2.

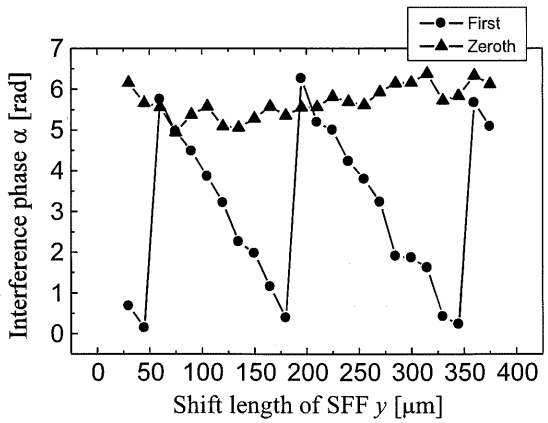

Fig. 8. The zeroth- and first-order interference phase variations.

Independent control of the interference phase creates the potential for new applications of interference measurements. For example, thicknesses smaller than the interference amplitude peak width can be measured by utilizing this phase control. The interference signal from a thin film with front and rear surfaces is expressed by $S(\Delta f, f_c)=B(L_1-c/\Delta f)\cos(\alpha_1)+B(L_2-c/\Delta f)\cos(\alpha_2)$, where $\alpha_1=2\pi L_1 f_c/c$ and $\alpha_2=2\pi L_2 f_c/c$. L_1 and L_2 are OPDs of the front and rear surfaces, respectively. If f_c is controlled to be equal to $[(1/4)+q]c/L_1$, where q is an integer, $S(\Delta f, f_c)=0+B(L_2-\Delta f)\cos(\alpha_2)$ is obtained. This means that the interference signal from the front surface disappears. Thus, while sweeping Δf to locate the rear surface, the interference signal from the front surface can be eliminated by controlling the fc. The same control of f_c can be obtained for the rear surface. We are currently investigating using this method to measure thickness profiles.

5. CONCLUSION

To summarize we confirmed the principle of multi-frequency sweeping interferometry, especially the relationship between the interference amplitude and the phase by using a novel multi-frequency light source which can sweep both the interval and center frequencies Symmetrically sweeping the interval frequency on either side of the center frequency produced a fixed interference phase while the interference amplitude was varied We demonstrated that the interference phase at the amplitude peak position can be arbitrarily controlled by sweeping the center frequency

ACKNOWLEDGEMENTS

This work was supported by a Grant-in-Aid for Young Scientists (B) (23760366)

REFERENCES

[1] K Minoshima and H Matsumoto, "High-Accuracy Measurement of 240-m Distance in an Optical Tunnel by use of a Compact Femtosecond Laser ' Appl Opt 39 5512–5517 (2000)

[2] K Joo and S Kim, "Absolute distance measurement by dispersive interferometry using a femtosecond pulse laser, Opt Express 14, 5954–5960 (2006)

[3] P Balling, P Kren, P Masika S V D Berg, "Femtosecond frequency comb based distance measurement in air ' Opt Express 17, 9300–9313 (2009)

[4] J Jinm, J W Kim, C Kang, J Kim, and T B Eom, "Thickness and refractive index measurement of a silicon wafer based on an optical comb," Opt Express 18 18339–18346 (2010)

[5] S Lee B Widiyatmoko, M Kourogi, and M Ohtsu, "Ultrahigh Scanning Speed Optical Coherence Tomography Using Optical Frequency Comb Generators, Jpn J Appl Phys 40, L878–L880 (2001)

[6] S Choi M Yamamoto, M Daisuke T Shioda, Y Tanaka and T Kurokawa "Frequency-comb-based interferometer for profilometry and tomography," Opt Lett 31, 1976–1978 (2006)

[7] S Choi N Tamura K Kashiwagi, T Shioda, Y Tanaka and T Kurokawa, "Supercontinuum Comb Generation Using Optical Pulse Synthesizer and Highly Nonlinear Dispersion-Shifted Fiber ' Jpn J Appl Phys 48 09LF01 (2009)

[8] O Sasaki, Y Ikeda T Suzuki, "Superluminescent Diode Interferometer Using Sinusoidal Phase Modulation for Step-Profile Measurement, ' Appl Opt 37, 5126–5131 (1998)